Am J Transl Res 2026;18(1):222-235
www.ajtr.org /ISSN:1943-8141/AJTR0169660

Original Article

MCT4 alleviates lipid accumulation, inflammation and PANoptosis in non-alcoholic fatty liver disease by inhibiting JAK-STAT signaling transduction

Bing Wu[1*], Hao Xu[2*], Yuqiao Zeng[2], Ao Shen[1], Cheng Zhang[1], Pengfei Wu[1], Xinyue Zhang[1], Han Zhang[1], Yiyu He[3], Likun Wang[2]

[1]School of Clinical Medicine, Shandong Second Medical University, Weifang 261053, Shandong, China; [2]Infection Control Center, Linyi People's Hospital, Linyi 276000, Shandong, China; [3]Department of Cardiovascular Disease, Renmin Hospital of Wuhan University, Wuhan 430060, Hubei, China. [*]Equal contributors and co-first authors.

Received October 29, 2025; Accepted December 9, 2025; Epub January 15, 2026; Published January 30, 2026

Abstract: Objectives: To investigate the role of monocarboxylate transporter 4 (MCT4) in non-alcoholic fatty liver disease (NAFLD) and its underlying mechanisms. Methods: Palmitic acid (PA) was used to stimulate L-02 cells, establishing an *in vitro* lipid accumulation model, and the effects of MCT4 overexpression on cell lipid accumulation, inflammatory response, and PANoptosis were analyzed. Mechanistically, the role of JAK1-STAT3 in NAFLD was explored by introducing the JAK1 activator Oncostatin. In addition, a NAFLD mouse model was established through a high-fat diet to validate the effects of MCT4 on liver lipid metabolism and inflammatory injury *in vivo*. Results: After PA treatment, the levels of triglycerides (TG), total cholesterol (TC), and low-density lipoprotein cholesterol (LDL-C) in cells increased, while the level of high-density lipoprotein cholesterol (HDL-C) decreased. The expression of lipid synthesis-related genes was upregulated, while the expression of lipid breakdown-related genes was downregulated. Similarly, PA induced cellular inflammatory infiltration and PANoptosis. However, overexpression of MCT4 reversed PA induced lipid accumulation and inflammatory response. Mechanistic studies demonstrated that MCT4 alleviated PA-induced lipid accumulation and inflammatory response by reducing the phosphorylation levels of JAK1 and STAT3. Compared with the model group, mice overexpressing MCT4 showed reduced liver tissue damage. Conclusions: MCT4 provides new reference for the treatment of NAFLD by inhibiting the JAK-STAT pathway, slowing down lipid accumulation and inflammatory response in NAFLD.

Keywords: Non-alcoholic fatty liver disease, monocarboxylate transporter 4, lipid accumulation, inflammation

Introduction

Non-alcoholic fatty liver disease (NAFLD) is a clinical pathological syndrome characterized by diffuse hepatic steatosis in the absence of alcohol consumption or other clear liver injury factors. It includes simple fatty liver disease and its progressive forms, including non-alcoholic steatohepatitis (NASH) and cirrhosis [1, 2]. NAFLD has long been the leading cause of chronic liver disease in developed Western countries, with a prevalence rate of 20%-40% among adults. NAFLD is also growing rapidly in Asian countries, with a prevalence of 14-15% in developed regions and showing a trend towards younger age groups [3, 4]. With the changes in dietary structure and lifestyle in China, the incidence of NAFLD has been increasing, making it the second most common liver disease after chronic viral hepatitis. Although generally considered a painless benign lesion, NAFLD carries a high risk of fibrosis. Therefore, actively seeking effective therapeutic strategies for NAFLD has become a hot research topic in recent years.

In the pathophysiological process of NAFLD, lactate is increasingly recognized as an important metabolite and signaling molecule, rather than just a metabolic waste. In NAFLD state, hepatic insulin resistance leads to abnormal glucose uptake and utilization, thereby enhancing glycolytic flux and producing excessive pyruvate. Due to impaired mitochondrial function

https://doi.org/10.62347/NFCT6486

or decreased oxidative capacity, pyruvate is converted to lactate by lactate dehydrogenase (LDH), leading to its hepatic accumulation. Lactic acid can promote the synthesis and accumulation of triglycerides (TG) in liver cells through a series of biochemical reactions [5]. Research has shown that both circulating and hepatic lactate levels are closely related to the progression of liver disease, with higher lactate levels indicating more severe liver disease progression [6-8]. Additionally, high acetylation of LDHB in the liver of NAFLD and NASH significantly reduces LDHB activity and impairs liver lactate clearance, leading to lactate accumulation, which further exacerbates liver lipid deposition and inflammatory response [9]. Another study showed that knocking down LDHA alleviated lipid accumulation, reduced TG and TC levels, and downregulated adipogenic proteins in the L-02 cell line treated with free fatty acids [10]. A cross-sectional analysis of NHANES data indicated a significant correlation between serum LDH levels, NAFLD, and advanced liver fibrosis, suggesting that LDH measurement has important clinical warning value for identifying high-risk patients, especially those with metabolic syndrome [11]. Collectively, abnormalities in lactate metabolism (including its production, transport, and utilization) are closely related to lipid deposition and inflammatory processes in NAFLD and may represent an important signaling mechanism driving NAFLD progression.

The monocarboxylate transporter (MCT) family is encoded by the solute transport protein family SLC16A gene, among which MCT1 and MCT4 are the most widely expressed and mediate transmembrane transport of lactate. At physiological pH, approximately 99% of lactic acid dissociates into anions and protons. Among them, MCT1 has a higher affinity for lactate in cells and is more inclined to uptake lactate from the extracellular environment, whereas MCT4 has a lower affinity for lactate and is more inclined to excrete lactate from the cell [12, 13]. A study found that in a NAFLD model induced by MCT1 haploinsufficiency mice, milder brain tissue damage was observed, suggesting a potential protective effect against NAFLD-associated neural changes despite the presence of steatosis [14]. Other studies have shown that MCT1 insufficiency promotes resistance to hepatic steatosis and inflammation [15]. Currently, research has focused on the role of MCT4 in NAFLD. Guo et al. showed that MCT4 overexpression downregulated lipogenic genes and upregulated lipid catabolism-associated genes. On the contrary, inhibiting MCT4 expression accelerated the accumulation of intracellular lipids and glucose metabolites, leading to hepatic steatosis. In vivo experiments further confirmed that exogenous MCT4 significantly alleviated hepatic steatosis in the NAFLD mouse model [16]. Although evidence suggests that MCT4 can promote lactate efflux, reshape the hepatic metabolic microenvironment, and exert anti-steatosis and anti-inflammatory effects, relevant studies remain limited. Therefore, targeting the MCT4 pathway provides a highly promising direction for developing novel therapies for NAFLD and is currently an active frontier in the field of metabolic liver disease research.

This study investigated the regulatory role of MCT4 in lipid accumulation and inflammatory response in NAFLD using both *in vivo* and *in vitro* experiments. Our research results may provide new insights into the pathogenesis of NAFLD.

Materials and methods

Cells and transfection

The human normal hepatocyte line L-02 was purchased from the Cell Bank of the Chinese Academy of Sciences (Shanghai, China). Cells were cultured in DMEM (Gibco, Rockville, MD) containing 10% (v/v) fetal bovine serum (Gibco, Australia), 100 U/mL penicillin and 100 μg/mL streptomycin at 37°C in an incubator containing 5% CO_2. An *in vitro* cellular steatosis model of NAFLD was established by stimulating L-02 cells with 0.25 mM palmitic acid (PA) for 24 hours. The pcDNA3.1-MCT4 overexpression plasmid was constructed by inserting the full-length human SLC16A3 cDNA (NCBI Reference Sequence: NM_004207.4) into the pcDNA3.1(+) vector (GeneCopoeia). A C-terminal FLAG tag was added for immunodetection. The construction was confirmed by Sanger sequencing. For transient transfection, cells were transfected with the plasmid using Lipofectamine 3000 (Thermo Fisher Scientific) according to the manufacturer's protocol.

Table 1. Primers for real-time RT-PCR

Gene	Primers	
	Forward (5'-3')	Reverse (5'-3')
MCT4	GTAGCAGGTATCCTTGAGACGG	TAAGTAGTGGAAATGTGGTGGC
LXRα	CTGATTCTGCAACGGAGTTGT	GACGAAGCTCTGTCGGCTC
FAS	CTGTCCTGCCTCTGGTGCTT	CAGCAAAATGGGCCTCCTT
ATGL	AACCAACCCAACCCTTTG	GTGGTCATCAGGTCTTTCG
HSL	CGCCTTACGGAGTCTATGC	TCTGATGGCTCTGAGTTGC
IL-6	GAGGATACCACTCCCAACAGACC	AAGTGCATCATCGTTGTTCATACA
IL-1β	CTTTCCCGTGGACCTTCCA	CTCGGAGCCTGTAGTGCAGTT
TNF-α	CTCCAGGCGGTGCCTATGT	GAAGAGCGTGGTGGCCC
IL-8	GGTAAAGTCCGTAAGTCGTAGTAC	AGTTAACGTGGAGGTACCGTA
ZBP1	GCAAACTCCGAAGCCATCCAGA	CCAAGTTGAGGAATCACCTGGTG
RIPK1	CTGGGCTTCACACAGTCTCA	GTCGATCCTGGAACACTGGT
GAPDH	GTCCCGAAAGAACTGGTG	CCAAAGCAATCAGGTAGCA

Animals

Twelve SPF-grade male C57BL/6J mice (18-22 g, 8 weeks) were purchased from the Wuhan Institute of Laboratory Animal Research. Mice were raised in an environment with alternating light and dark for 12 hours and were free to drink water. After adaptive feeding, all mice were randomly divided into the control group (n=3) and the model group (n=9). The model group mice were further divided into three groups (n=3 in each group): the NAFLD model group, the negative control group, and the treatment group. The control group was given normal feed, while the model group was fed a 60% high-fat diet to establish the disease model. The negative control group was injected with empty plasmid through the tail vein, while the treatment group was injected with MCT4 overexpression plasmid. Rats were euthanized by intraperitoneal injection of an overdose of sodium pentobarbital (150 mg/kg). Death was confirmed by the absence of respiration, cessation of heartbeat (verified by auscultation), and loss of corneal reflex, in accordance with the AVMA Guidelines for the Euthanasia of Animals (2020 Edition). Then, the peripheral blood and liver tissues were collected for subsequent analysis. This study was approved by the Animal Ethics Committee of Linyi People's Hospital.

RT-qPCR

Total RNA was extracted using Trizol reagent (Invitrogen, USA) and reverse transcribed into cDNA using PrimeScript reverse transcription kit (Takara, China). The reverse transcription reaction system was 10 μL, carried out at 37°C, and was cycled three times for 15 minutes each time. The resulting cDNA was then used as template in real-time PCR amplification (Applied Biosystems, Carlsbad, CA). Gene expression levels were analyzed using the 2-ΔΔCt method with normalization to reference genes. All primers were designed and synthesized by Sangon Biotech (Shanghai, China) (**Table 1**).

Western blotting

Samples to be tested were collected and lysed to extract total protein. The extracted proteins were separated by SDS-PAGE and subsequently transferred onto PVDF membranes (Bio-Rad, California, USA). The membrane containing protein was blocked with 5% skimmed milk powder at room temperature for 2 hours, followed by incubation with primary antibody overnight at 4°C. The primary antibodies (Abcam, UK) included GAPDH (1:500), MCT4 (1:600), JAK1 (1:1000), phosphorylated JAK1 (Y1034+Y1035, 1:1000), STAT3 (1:2000), and phosphorylated STAT3 (Y705, 1:3000). The next day, the membrane was rinsed with PBS, followed by incubation with the corresponding secondary antibodies at room temperature. Finally, the protein bands were developed using the enhanced chemiluminescence (ECL) method (Pierce, Rockford, IL, USA), and the expression levels of the proteins were quantified using the ImageJ software (National Institutes of Health, USA).

ELISA

The concentrations of key cytokines, including tumor necrosis factor-alpha (TNF-α), interleukin-1 beta (IL-1β), interleukin-6 (IL-6) and IL-8, in cell supernatants were determined by ELISA using kits from Solarbio (China), according to the manufacturer's protocol.

Measurement of biochemical parameters

The levels of triglycerides (TG), total cholesterol (TC), low-density lipoprotein cholesterol (LDL-

C), high-density lipoprotein cholesterol (HDL-C), aspartate aminotransferase (AST), and alanine aminotransferase (ALT) were detected using relevant kits (Sigma). All determinations were carried out on fully automatic biochemical analyzers, and the corresponding concentrations were calculated through standard curves.

Oil red O staining

Liver tissue sections were prepared and air-dried for 15 min at room temperature. Sections were sequentially incubated in 100% isopropanol for 5 min, then in 0.5% oil red O solution at 60°C for 8 min, followed by a 3-min wash in 85% isopropanol and counterstaining with hematoxylin for 2 min. Lipid droplet accumulation was assessed based on staining intensity, and the average number of red droplets per cell was quantified using ImageJ software (National Institutes of health, USA).

Tissue hematoxylin and eosin (H&E) staining

Liver tissue slices were fixed with 4% paraformaldehyde solution for 48 hours, followed by decalcification treatment using 20% buffered EDTA solution. Afterwards, the tissue was embedded in paraffin, stained with hematoxylin and eosin (Sigma-Aldrich, St. Louis, Missouri), and observed and photographed under a microscope (Olympus IX71; Tokyo, Japan). For quantitative histopathological analysis, digital images of H&E-stained sections were analyzed using ImageJ software (National Institutes of Health, USA). Regions of interest (areas showing inflammatory infiltration, necrosis, or steatosis) were manually delineated by an observer blinded to this study, and the percentage of affected area relative to the total tissue area was calculated.

Immunohistochemical assay

After antigen retrieval, tissue regions were circled and non-specific binding sites were blocked. The tissue sections were then incubated with primary antibody (Abcam, UK) working solution overnight at 4°C in a humid chamber. The next day, the slices were equilibrated to room temperature for 30 minutes, washed three times with distilled water, and then incubated with the secondary antibody working solution for 10 minutes. Subsequently, color development was performed using 3,3'-diaminobenzidine under dark conditions. After the color development was completed, sections were counterstained with hematoxylin and differentiated with hydrochloric acid ethanol. Finally, sections were rinsed, observed under an optical microscope (Olympus Corporation, Japan) and photographed using ImageJ/Fiji (National Institutes of Health, USA).

Flow cytometry

Cell culture supernatant was collected and washed with PBS buffer. The cells were resuspended and adjusted to a density of 2×10^4 cells/mL. Next, 100 μL of the cell suspension was inoculated into the culture container. Cells were then incubated with annexin V-FITC and propidium iodide in the dark. Finally, binding buffer was added to the tube, and apoptosis rate was analyzed by flow cytometry.

Statistical analysis

SPSS 22.0 was used for all data analyses. Normally distributed measurement data were presented as means ± standard deviation. Comparisons between the two groups were analyzed using t-tests, and among multiple groups were conducted using one-way ANOVA followed by LSD test. A P value of <0.05 indicated statistical significance.

Results

MCT4 expression was reduced in the livers of NAFLD mice

Immunohistochemistry and RT-qPCR analyses revealed that MCT4 expression was decreased in liver tissues of NAFLD mice (**Figure 1A**, **1B**), suggesting that dysregulated MCT4 expression may be closely associated with NAFLD progression. However, in the *in vitro* NAFLD model established by treating L-02 cells with 0.25 mM palmitic acid (PA) for 24 hours, MCT4 mRNA expression was increased- contrary to the *in vivo* findings (**Figure 1C**). We speculate that the downregulation of MCT4 in NAFLD mouse liver tissues reflects chronic metabolic dysfunction and impaired hepatocyte function, whereas the upregulation of MCT4 mRNA in PA-treated L-02 cells may represent an acute stress or compensatory response, whereby MCT4 responds to early lipid accumulation induced by PA. Subsequently, we transfected L-02 cells with

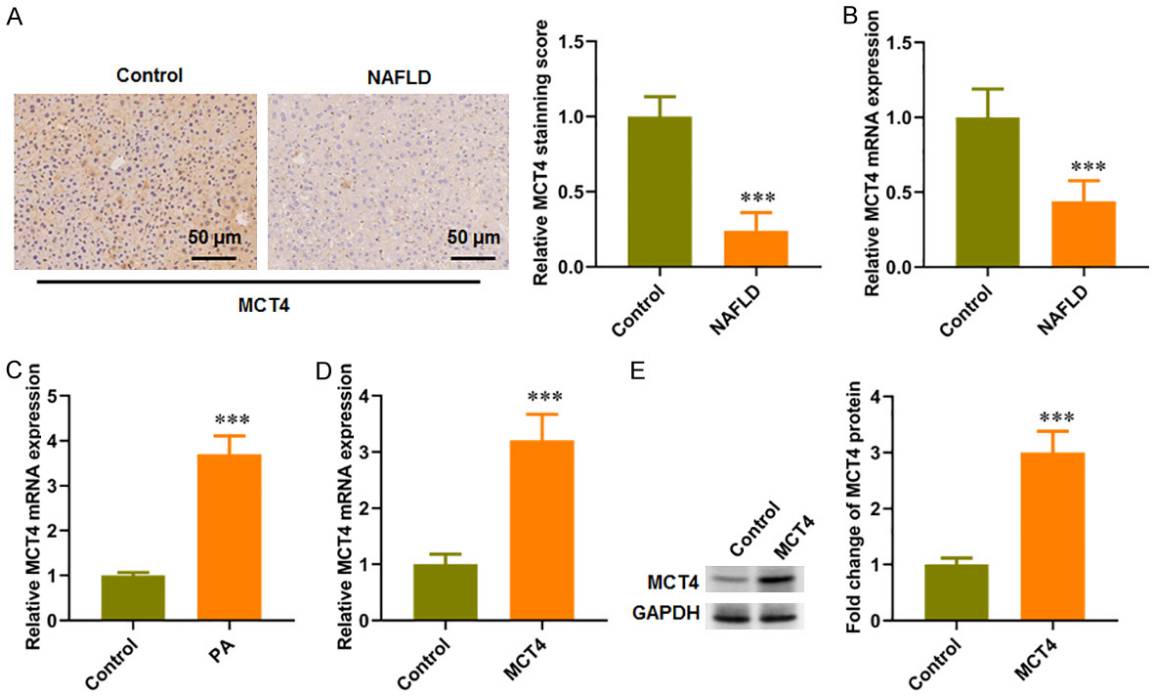

Figure 1. Expression levels of MCT4 in NAFLD. A, B. Expression levels of MCT4 in liver tissues of NAFLD mice, as determined by immunohistochemistry and RT-qPCR. L-02 cells were treated with 0.25 mM palmitic acid (PA) for 24 hours to establish an *in vitro* cellular model of NAFLD. C. The mRNA expression of MCT4 in PA-treated L-02 cells. D, E. Validation of MCT4 overexpression plasmid transfection efficiency by detecting mRNA and protein expression levels of MCT4. Scale bar =50 μm. N=3. ***P<0.001.

an MCT4 overexpression plasmid, and both mRNA (**Figure 1D**) and protein levels (**Figure 1E**) of MCT4 were significantly increased, confirming efficient transfection.

MCT4 inhibited PA-induced lipid accumulation in cells

L-02 cells were treated with 0.25 mM PA for 24 hours, and the levels of TG, TC, LDL-C, and HDL-C were detected. Compared with the Control group, the contents of TG, TC, and LDL-C in the PA group cells were significantly increased, while the content of HDL-C was decreased, indicating an increase in lipid accumulation in the cells. After overexpression of MCT4, the levels of TG, TC, and LDL-C (**Figure 2A-C**) were decreased, while the level of HDL-C (**Figure 2D**) was increased, indicating that MCT4 mitigated lipid accumulation. In addition, we detected the expression of lipid metabolism-related genes and found that PA significantly promoted the expression of lipid synthesis genes LXRα (**Figure 2E**) and FAS (**Figure 2F**), while inhibiting the expression of lipolytic genes ATGL (**Figure 2G**) and HSL (**Figure 2H**), indicating enhanced lipid synthesis and reduced lipid breakdown. However, this effect was reversed after MCT4 overexpression.

MCT4 inhibited PA-induced cellular inflammation

After treatment with 0.25 mM PA for 24 hours, the secretion levels of inflammatory factors IL-6, IL-1β, TNF-α, and IL-8 in L-02 cells significantly increased compared to the control group (**Figure 3A-D**). Similarly, the mRNA expression of IL-6, IL-1β, TNF-α, and IL-8 was increased following PA treatment, while overexpression of MCT4 reversed the promoting effect of PA on inflammatory response (**Figure 3E-H**), indicating that MCT4 can inhibit PA induced cellular inflammatory response.

MCT4 inhibited PA-induced PANoptosis

Inflammation and lipid accumulation are the key triggers of PANoptosis, which often cause cell death in synergy, leading to the aggravation of tissue damage in a variety of metabolic and infectious diseases. In the cells treated with

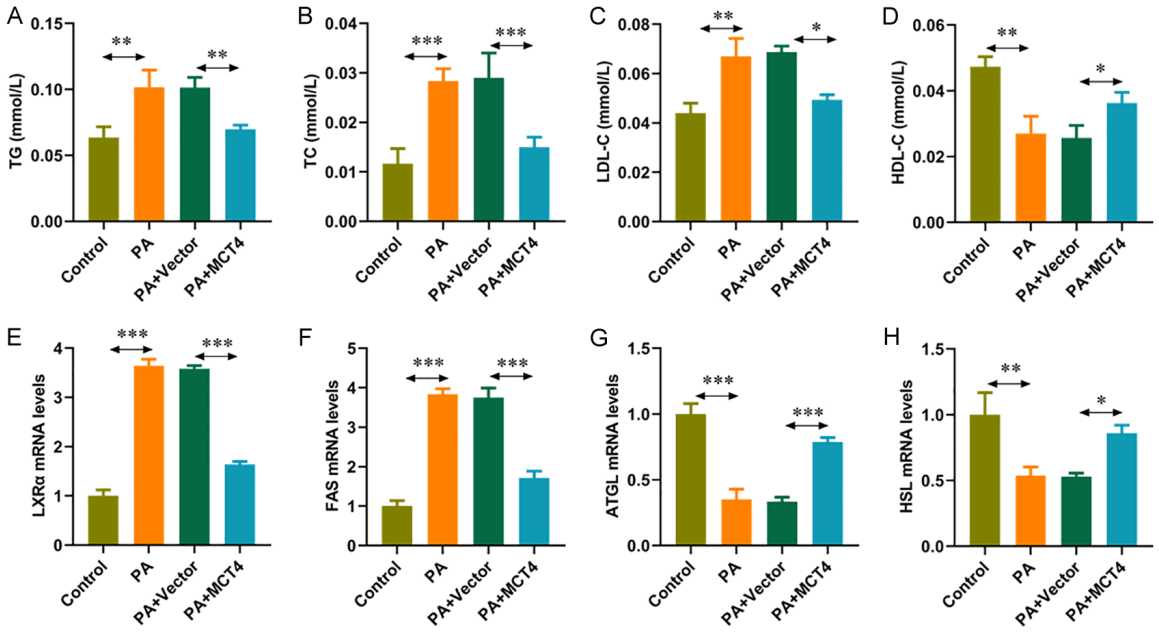

Figure 2. Effects of MCT4 on cellular lipid accumulation. A. Intracellular triglyceride (TG) content. B. Intracellular total cholesterol (TC) content. C, D. Intracellular low-density lipoprotein cholesterol (LDL-C) and high-density lipoprotein cholesterol (HDL-C) levels. E-H. The mRNA expression levels of lipogenic genes (LXRα, FAS) and lipolytic genes (ATGL, HSL). N=3. **P*<0.05. ***P*<0.01. ****P*<0.001.

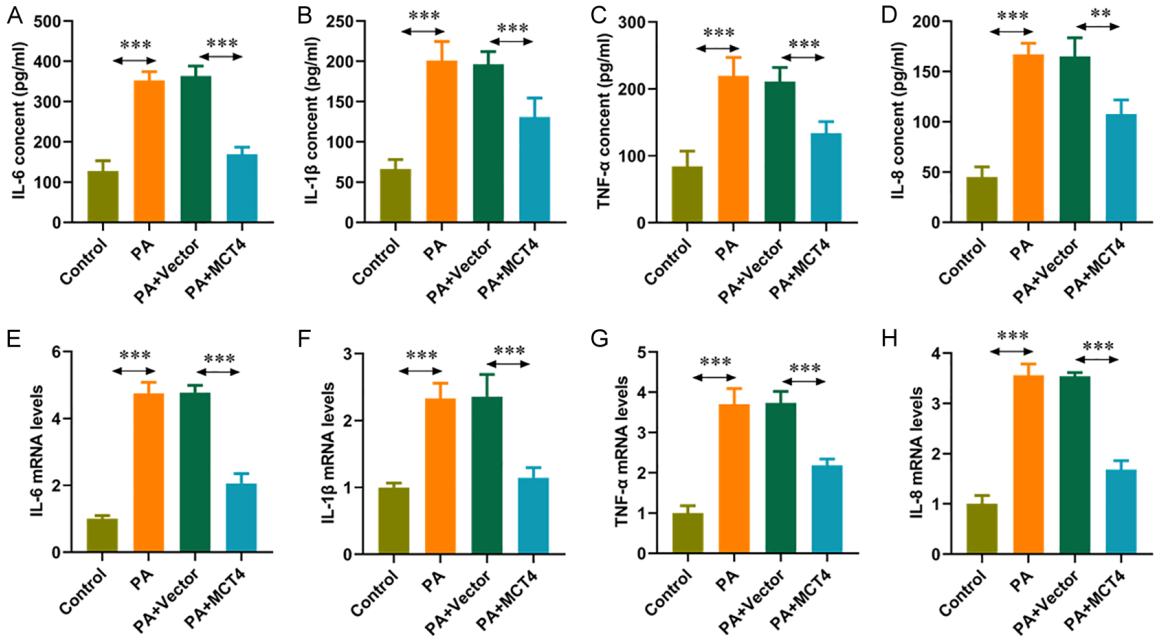

Figure 3. Effects of MCT4 on cellular inflammatory response. A, E. Secretion and mRNA levels of IL-6. B, F. Secretion and mRNA levels of TNF-α. C, G. Secretion and mRNA levels of IL-1β. D, H. Secretion and mRNA levels of IL-8. N=3. ***P*<0.01. ****P*<0.001.

PA, the levels of cleaved Caspase-3, cleaved Caspase-1, and phosphorylated MLKL increased, indicating induction of PANoptosis, while MCT4 transfection inhibited PA induced PANoptosis (**Figure 4A-C**). Meanwhile, PA upregulated the expression of PANoptosis related pro-

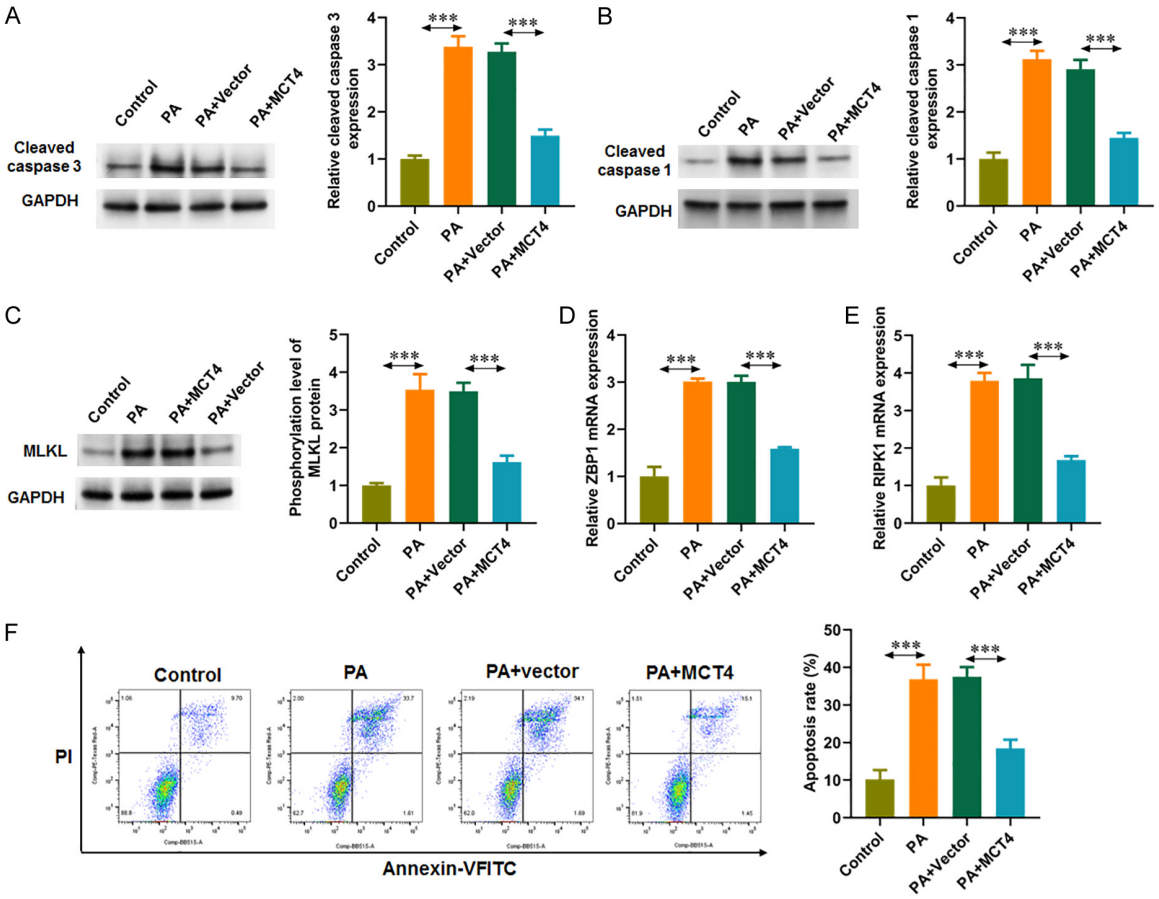

Figure 4. Effects of MCT4 on cell apoptosis. A-C. The expression of cleaved caspase 3, cleaved caspase 1 and MLKL. D, E. The mRNA expression levels of PANoptosome-associated molecules ZBP1 and RIPK1. F. Cell apoptosis. N=3. ***P<0.001.

teins ZBP1 and RIPK1 (**Figure 4D**, **4E**), and increased cell apoptosis (**Figure 4F**), while overexpression of MCT4 reduced the levels of these molecules and alleviated cell apoptosis.

MCT4 inhibited PA-induced JAK1-STAT3 pathway activation

PA significantly activated the JAK1-STAT3 signaling pathway, while transfection of MCT4 reduced JAK1 and STAT3 protein phosphorylation levels. However, intervention with JAK1 activator Oncostatin M (OSM) reactivated this pathway (**Figure 5A**). Regarding the role of the AK1-STAT3 pathway in PA-induced lipid accumulation and inflammation, MCT4 significantly reduced the levels of TG, TC, and LDL-C (**Figure 5B-D**) in PA-treated cells, but these inhibitory effects were eliminated by OSM, which promoted lipogenic gene LXRα and inhibited mRNA expression of lipolytic gene HSL (**Figure 5E**, **5F**). In addition, PA increased the secretion of IL-6, TNF-α, and IL-1β (**Figure 5G-I**), while MCT4 overexpression attenuated the inflammatory response. However, OSM restored cytokine secretion, indicating that MCT4 reduces lipid accumulation and inflammation in PA-treated L-02 cells by inhibiting the JAK1-STAT3 signaling pathway. Inflammation and lipid accumulation are key triggers of PANoptosis, often acting synergistically to promote cell death and exacerbate tissue damage in metabolic and infectious diseases. In PA-treated L-02 cells, the expression of PANoptosome components ZBP1, RIPK1, and AIM2 was elevated; However, MCT4 overexpression reduced their levels and this was restored after JAK1 activation via OSM (**Figure 5J-L**). This suggests PANoptosis is involved in PA-driven inflammatory and lipotoxic processes.

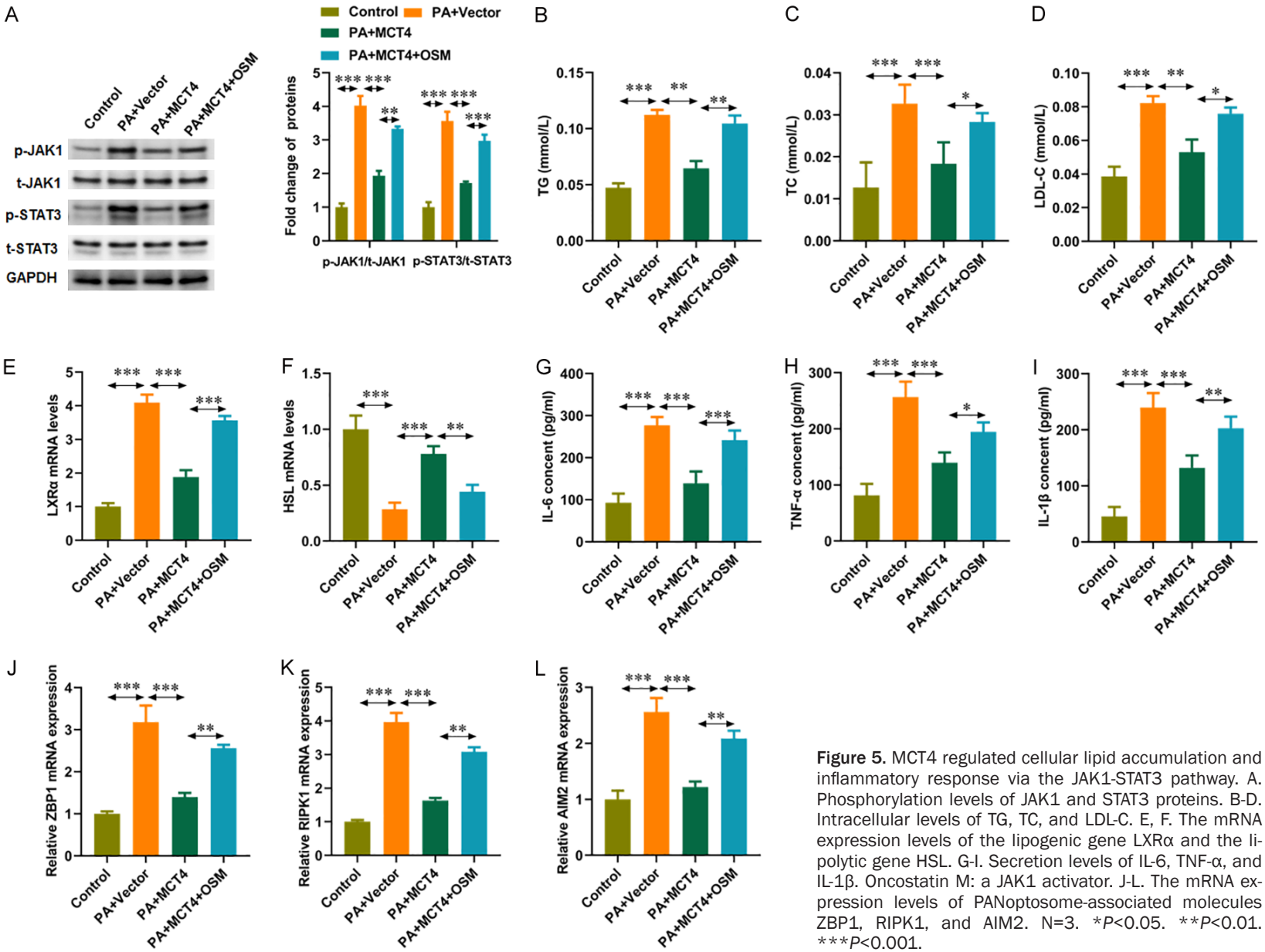

Figure 5. MCT4 regulated cellular lipid accumulation and inflammatory response via the JAK1-STAT3 pathway. A. Phosphorylation levels of JAK1 and STAT3 proteins. B-D. Intracellular levels of TG, TC, and LDL-C. E, F. The mRNA expression levels of the lipogenic gene LXRα and the lipolytic gene HSL. G-I. Secretion levels of IL-6, TNF-α, and IL-1β. Oncostatin M: a JAK1 activator. J-L. The mRNA expression levels of PANoptosome-associated molecules ZBP1, RIPK1, and AIM2. N=3. **P*<0.05. ***P*<0.01. ****P*<0.001.

MCT4 alleviated hepatic lipid accumulation and injury in NAFLD mice

Compared with the control group, mice in the NAFLD group showed increased liver weight and index, indicating successful mouse modeling. After administration of MCT4, the liver weight (**Figure 6A**) and liver index (**Figure 6B**) of mice decreased, suggesting a protective effect against HFD-induced hepatic injury. In this study, serum levels of AST and ALT in NAFLD mice increased, whereas MCT4 overexpression decreased these levels (**Figure 6C**, **6D**). Similarly, hepatic TG and TC levels were lower in MCT4-overexpressing mice than those in NAFLD mice (**Figure 6E**, **6F**). Analysis of inflammatory cytokines showed that IL-6 (**Figure 6G**) and TNF-α (**Figure 6H**) levels in the liver of NAFLD mice were increased, while overexpression of MCT4 reduced the levels of these inflammatory cytokines. Immunohistochemistry and Western blotting showed reduced MCT4 expression and increased phosphorylation levels of JAK1 and STAT3 in the liver of NAFLD mice, which were reversed by MCT4 overexpression (**Figure 6I**, **6J**). A large number of red lipid droplets positive for oil red O staining were observed in the liver tissues of NAFLD mice, while in the MCT4 overexpression group, the number of lipid droplets decreased (**Figure 6K**). The HE staining results of liver tissues in the NAFLD mice showed that lipid deposition formed vacuoles in the liver tissues, and the structure of liver lobules was damaged. The number of vacuoles in the liver tissues in the MCT4 overexpression group decreased, and hepatocytes were arranged radially around the central vein (**Figure 6L**).

Discussion

Under physiological conditions, the steady-state concentration of TG in the liver is very low, accounting for approximately 5% of total liver volume. However, when the accumulation rate of fatty acids exceeds their clearance rate, excessive fatty acids are stored in lipid droplets, a process clinically defined as hepatic steatosis [17, 18]. Current research indicates that fat accumulation in the liver and persistent chronic inflammation are major triggers of NAFLD. Therefore, preventing excessive hepatic fat accumulation and controlling oxidative stress have become effective means for the prevention and treatment of NAFLD.

Our research indicates that MCT4 expression is downregulated in both PA-induced liver cell and HFD-fed NAFLD mouse models, whereas its overexpression improves liver steatosis and inflammation. These findings position MCT4 as a novel regulator of lipid metabolism and inflammatory signaling in NAFLD. It is worth noting that MCT4 overexpression reversed PA-induced accumulation of TG, TC, and LDL-C, while restoring HDL-C levels and rebalancing the expression of adipogenic and lipolytic genes. This metabolic improvement is consistent with recent reports indicating that monocarboxylate transporters affect cellular energy flux and redox balance, which are known to regulate de novo adipogenesis [19, 20]. Importantly, unlike previous studies that focused on MCT1 or MCT2 in liver metabolism, our work links MCT4 with the pathogenesis of NAFLD. Meanwhile, MCT4 inhibits the secretion of pro-inflammatory cytokines (TNF-α, IL-1β, IL-6) *in vitro* and reduces liver inflammatory infiltration *in vivo*. Under normal physiological conditions, inflammatory cytokines are almost rarely present in the liver. However, pathological stimuli such as lipid accumulation can induce hepatocytes to produce inflammatory cytokines, leading to chronic inflammatory infiltration, necrosis, apoptosis and fibrosis, thereby promoting the development and deterioration of NAFLD [21, 22]. Compared with normal livers, TNF-α and TNF receptor expression in the livers of NAFLD patients is increased, and even higher in NASH patients [23, 24]. Similarly, IL-6 levels are consistently higher in NAFLD/NASH patients [25]. Although the elevation of TNF and IL-6 has been well documented in human NASH, our data extends these observations by linking their production to reduced MCT4, which was previously not established.

Mechanistically, we observed overactivation of the JAK1-STAT3 pathway in the NAFLD model, and overexpression of MCT4 effectively alleviated this overactivation. This is consistent with emerging evidence that JAK-STAT signaling integrates metabolic and inflammatory cues in fatty liver disease [26, 27]. According to reports, the progression of NASH can be inhibited by miR-142-5p overexpression, which relies on the inhibition of thymic stromal lymphopoietin and JAK-STAT signaling pathways [28]. In addition, interruption of hepatic GH-JAK2-STAT5 signaling pathway is associated with lipid metabolism in both human and mouse NAFLD models [29].

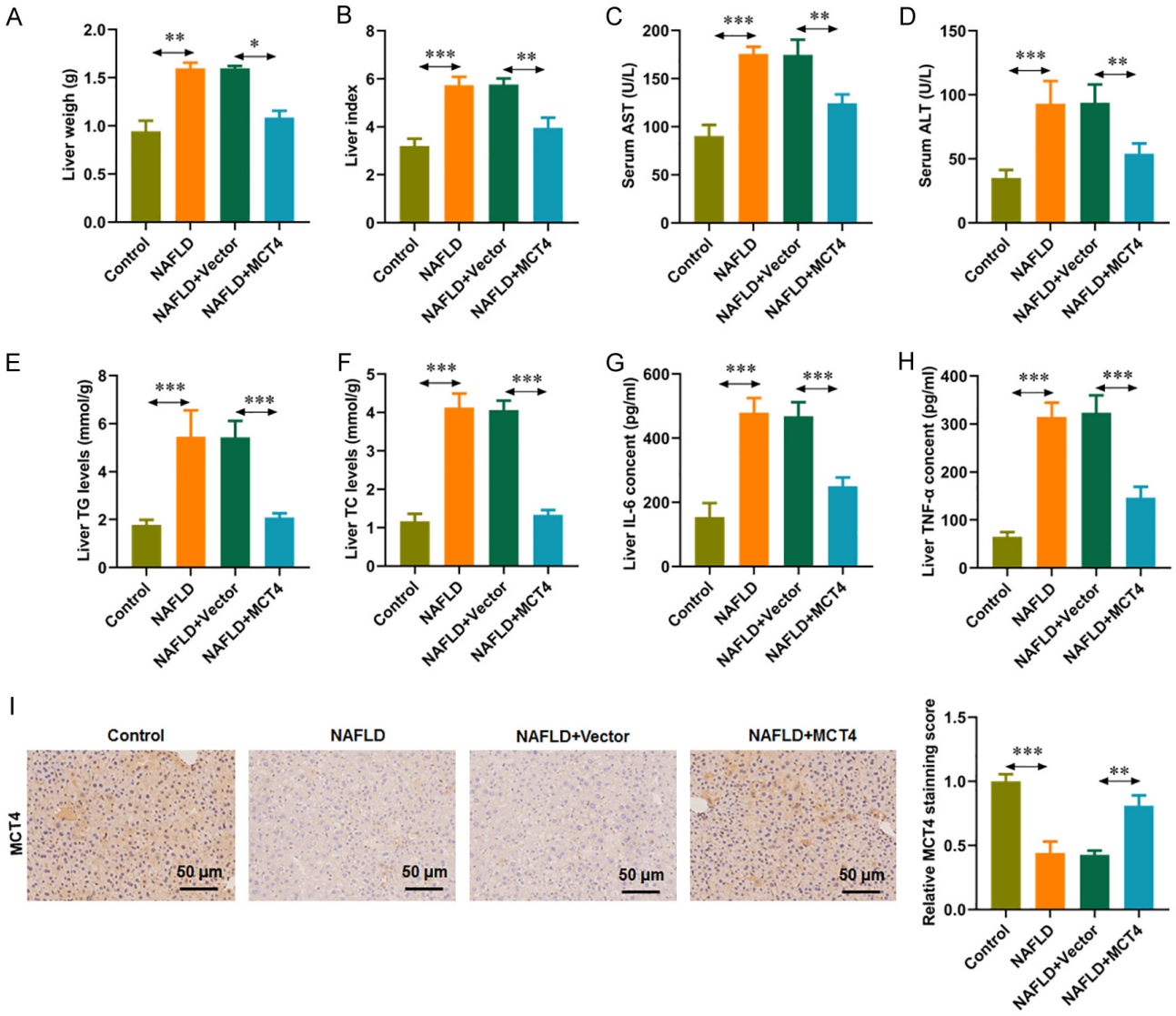
A
Liver weigh (g)
B
Liver index
C
Serum AST (U/L)
D
Serum ALT (U/L)
E
Liver TG levels (mmol/g)
F
Liver TC levels (mmol/g)
G
Liver IL-6 concent (pg/ml)
H
Liver TNF-α concent (pg/ml)
I
MCT4
Control
NAFLD
NAFLD+Vector
NAFLD+MCT4
50 μm
Relative MCT4 stainning score

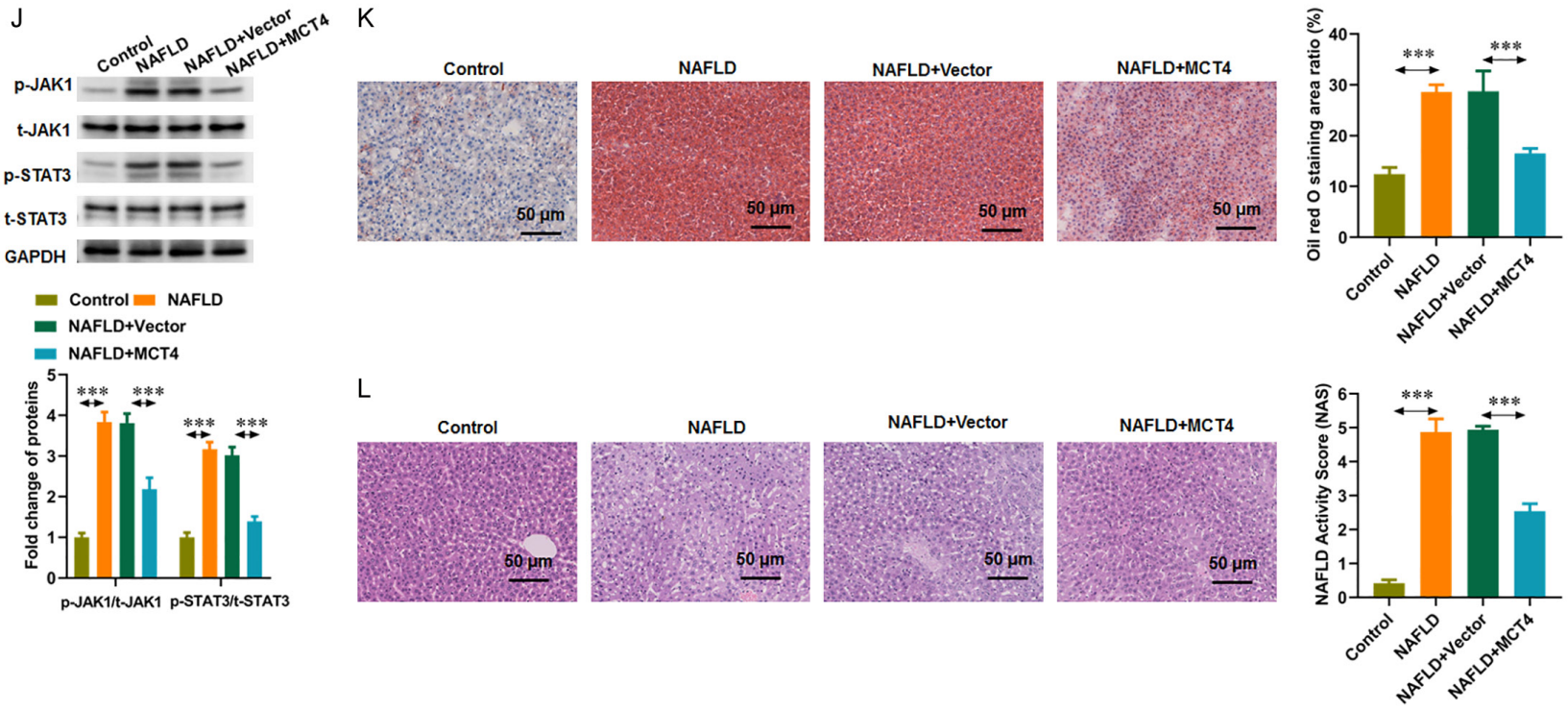

Figure 6. Therapeutic effects of MCT4 in NAFLD mice. A, B. Liver wet weight and liver index. C, D. Serum levels of AST and ALT. E, F. Hepatic levels of TG and TC. G, H. Secretion levels of IL-6 and TNF-α in liver tissues. I. Representative images of MCT4 immunohistochemistry. J. Phosphorylation levels of JAK1 and STAT3 proteins. K. Oil Red O staining showing lipid droplet accumulation in liver tissues. L. Hematoxylin and eosin staining images of liver tissues. Scale bar =50 μm. N=3. **P*<0.05. ***P*<0.01. ****P*<0.001.

It has also been reported that natural killer cells are activated in the liver of NASH, in a more pro-inflammatory cytokine environment, and promote the development of NASH through the cytokine -JAK-STAT1/3 axis [30]. Research has shown that blockade of the JAK-STAT signaling pathway is associated with P38γ inhibition, which helps reduce lipid accumulation in AML-12 cells induced by free fatty acids [31]. Based on the above research background, it is confirmed that JAK-STAT plays an important role in NAFLD.

Despite these findings, our research still has limitations. First, although the L-02 cell line is widely used, it belongs to the immortalized cell line and may not fully reproduce the behavior of primary human liver cells. Second, we did not investigate whether the role of MCT4 depends on its canonical transport function or involves non-classical signaling functions. Future research should employ hepatocyte-specific MCT4 knockout mice and evaluate their therapeutic potential in advanced NAFLD models with fibrosis.

Conclusion

MCT4 expression is reduced during the progression of NAFLD, and its loss contributes to lipid metabolism disorders and inflammatory damage in the liver. Further research shows that MCT4 can block the JAK1-STAT3 signaling pathway to alleviate hepatocellular steatosis and inflammation of hepatocytes in NAFLD. Therefore, MCT4 may be a potential therapeutic target for NAFLD.

Acknowledgements

This study was supported by the Natural Science Foundation of Shandong Province (No. ZR2021MH375), and the TCM Science and Technology Key Project of Shandong Province (No. Z-2022036).

Disclosure of conflict of interest

None.

Abbreviations

NAFLD, non-alcoholic fatty liver disease; MCT4, monocarboxylate transporter 4; TG, triglycerides; TC, total cholesterol; LDL-C, low-density lipoprotein cholesterol; HDL-C, high-density lipoprotein cholesterol; PA, palmitic acid; NASH, non-alcoholic steatohepatitis; LDH, lactate dehydrogenase; MCT, monocarboxylate transporter; HFD, high-fat diet; JAK, Janus kinase; STAT, signal transducer and activator of transcription.

Address correspondence to: Yiyu He, Department of Cardiovascular Disease, Renmin Hospital of Wuhan University, No. 238 Jiefang Road, Wuchang District, Wuhan 430060, Hubei, China. E-mail: Heyiyu09160@126.com; Likun Wang, Infection Control Center, Linyi People's Hospital, No. 27 Jiefang Road, Lanshan District, Linyi 276000, Shandong, China. E-mail: Lkwang999@163.com

References

[1] Isaacs S. Nonalcoholic fatty liver disease. Endocrinol Metab Clin North Am 2023; 52: 149-164.
[2] Ding L, Oligschlaeger Y, Shiri-Sverdlov R and Houben T. Nonalcoholic fatty liver disease. Handb Exp Pharmacol 2022; 270: 233-269.
[3] Teng ML, Ng CH, Huang DQ, Chan KE, Tan DJ, Lim WH, Yang JD, Tan E and Muthiah MD. Global incidence and prevalence of nonalcoholic fatty liver disease. Clin Mol Hepatol 2023; 29: S32-s42.
[4] Dai JJ, Zhang YF and Zhang ZH. Global trends and hotspots of treatment for nonalcoholic fatty liver disease: a bibliometric and visualization analysis (2010-2023). World J Gastroenterol 2023; 29: 5339-5360.
[5] Yao S, Chai H, Tao T, Zhang L, Yang X, Li X, Yi Z, Wang Y, An J, Wen G, Jin H and Tuo B. Role of lactate and lactate metabolism in liver diseases (Review). Int J Mol Med 2024; 54: 59.
[6] Hong W, Zeng X, Wang H, Tan X, Tian Y, Hu H, Ashrafizadeh M, Sethi G, Huang H and Duan C. PGC-1α loss promotes mitochondrial protein lactylation in acetaminophen-induced liver injury via the LDHB-lactate axis. Pharmacol Res 2024; 205: 107228.
[7] Li Q, Zhang F, Wang H, Tong Y, Fu Y, Wu K, Li J, Wang C, Wang Z, Jia Y, Chen R, Wu Y, Cui R, Wu Y, Qi Y, Qu K, Liu C and Zhang J. NEDD4 lactylation promotes APAP induced liver injury through caspase11 dependent non-canonical pyroptosis. Int J Biol Sci 2024; 20: 1413-1435.
[8] Ma YL, Ke JF, Wang JW, Wang YJ, Xu MR and Li LX. Blood lactate levels are associated with an increased risk of metabolic dysfunction-associated fatty liver disease in type 2 diabetes: a real-world study. Front Endocrinol (Lausanne) 2023; 14: 1133991.

[9] Wang T, Chen K, Yao W, Zheng R, He Q, Xia J, Li J, Shao Y, Zhang L, Huang L, Qin L, Xu M, Zhang Z, Pan D, Li Z and Huang F. Acetylation of lactate dehydrogenase B drives NAFLD progression by impairing lactate clearance. J Hepatol 2021; 74: 1038-1052.
[10] Meng J, Yan C and Liu J. LDHA- mediated histone lactylation promotes the nonalcoholic fatty liver disease progression through targeting the METTL3/YTHDF1/SCD1 m6A axis. Physiol Res 2024; 73: 985-999.
[11] Zhang X, Liu M, Huang J, Zheng Y, Wang Y and Zhou Y. Association of serum lactate dehydrogenase levels with non-alcoholic fatty liver disease and advanced hepatic fibrosis in the United States: a cross-sectional study using NHANES data from 2007 to 2018. BMC Gastroenterol 2025; 25: 467.
[12] Felmlee MA, Jones RS, Rodriguez-Cruz V, Follman KE and Morris ME. Monocarboxylate transporters (SLC16): function, regulation, and role in health and disease. Pharmacol Rev 2020; 72: 466-485.
[13] Luo X, Li Z, Chen L, Zhang X, Zhu X, Wang Z and Chen Y. Monocarboxylate transporter 1 in the liver modulates high-fat diet-induced obesity and hepatic steatosis in mice. Metabolism 2023; 143: 155537.
[14] Hadjihambi A, Konstantinou C, Klohs J, Monsorno K, Le Guennec A, Donnelly C, Cox IJ, Kusumbe A, Hosford PS, Soffientini U, Lecca S, Mameli M, Jalan R, Paolicelli RC and Pellerin L. Partial MCT1 invalidation protects against diet-induced non-alcoholic fatty liver disease and the associated brain dysfunction. J Hepatol 2023; 78: 180-190.
[15] Min K, Yenilmez B, Kelly M, Echeverria D, Elleby M, Lifshitz LM, Raymond N, Tsagkaraki E, Harney SM, DiMarzio C, Wang H, McHugh N, Bramato B, Morrison B, Rothstein JD, Khvorova A and Czech MP. Lactate transporter MCT1 in hepatic stellate cells promotes fibrotic collagen expression in nonalcoholic steatohepatitis. Elife 2024; 12: RP89136.
[16] Gou Y, Li A, Dong X, Hao A, Li J, Xiang H, Rahaman S, He TC and Fan J. Lactate transporter MCT4 regulates the hub genes for lipid metabolism and inflammation to attenuate intracellular lipid accumulation in non-alcoholic fatty liver disease. Genes Dis 2025; 12: 101554.
[17] Seebacher F, Zeigerer A, Kory N and Krahmer N. Hepatic lipid droplet homeostasis and fatty liver disease. Semin Cell Dev Biol 2020; 108: 72-81.
[18] Heeren J and Scheja L. Metabolic-associated fatty liver disease and lipoprotein metabolism. Mol Metab 2021; 50: 101238.
[19] Zhang Y, Li L, Li Y, Fei Y, Xue C, Yao X, Zhao Y, Wang X, Li M and Luo Z. An ROS-activatable nanoassembly remodulates tumor cell metabolism for enhanced ferroptosis therapy. Adv Healthc Mater 2022; 11: e2101702.
[20] Han J, Zhao C, Guo H, Liu T, Li Y, Qi Y, Deussing JM, Zhang Y, Tan J, Han H and Ma X. Obesity induces male mice infertility via oxidative stress, apoptosis, and glycolysis. Reproduction 2023; 166: 27-36.
[21] Mounika N, Mungase SB, Verma S, Kaur S, Deka UJ, Ghosh TS and Adela R. Inflammatory protein signatures as predictive disease-specific markers for non-alcoholic steatohepatitis (NASH). Inflammation 2025; 48: 25-41.
[22] Wei Z, Xue Y, Xue Y, Cheng J, Lv G, Chu L, Ma Z and Guan S. Ferulic acid attenuates non-alcoholic steatohepatitis by reducing oxidative stress and inflammation through inhibition of the ROCK/NF-κB signaling pathways. J Pharmacol Sci 2021; 147: 72-80.
[23] Duan Y, Pan X, Luo J, Xiao X, Li J, Bestman PL and Luo M. Association of inflammatory cytokines with non-alcoholic fatty liver disease. Front Immunol 2022; 13: 880298.
[24] Li J, Wang T, Liu P, Yang F, Wang X, Zheng W and Sun W. Hesperetin ameliorates hepatic oxidative stress and inflammation via the PI3K/AKT-Nrf2-ARE pathway in oleic acid-induced HepG2 cells and a rat model of high-fat diet-induced NAFLD. Food Funct 2021; 12: 3898-3918.
[25] Zhou W, Zhu Z, Xiao X, Li C, Zhang L, Dang Y, Ge G, Ji G, Zhu M and Xu H. Jiangzhi Granule attenuates non-alcoholic steatohepatitis by suppressing TNF/NFκB signaling pathway-a study based on network pharmacology. Biomed Pharmacother 2021; 143: 112181.
[26] Ou X, Chen J, Li B, Yang Y, Liu X, Xu Z, Xiang X and Wang Q. Multiomics reveals the ameliorating effect and underlying mechanism of aqueous extracts of polygonatum sibiricum rhizome on obesity and liver fat accumulation in high-fat diet-fed mice. Phytomedicine 2024; 132: 155843.
[27] Xiaoyu YU, Sun Y, Wang C, Wang Y, Hao R and Sun H. Recombinant hirudin prevents against nonalcoholic fatty liver disease by modulating PAR1/JAK2/STAT5/STAT3/CD36 pathway. Biochim Biophys Acta Mol Cell Biol Lipids 2025; 1870: 159678.
[28] Zhou C, Wang P, Lei L, Huang Y and Wu Y. Overexpression of miR-142-5p inhibits the progression of nonalcoholic steatohepatitis by targeting TSLP and inhibiting JAK-STAT signaling pathway. Aging (Albany NY) 2020; 12: 9066-9084.
[29] Kaltenecker D, Themanns M, Mueller KM, Spirk K, Suske T, Merkel O, Kenner L, Luís A, Kozlov A, Haybaeck J, Müller M, Han X and Moriggl R. Hepatic growth hormone - JAK2 -

STAT5 signalling: metabolic function, non-alcoholic fatty liver disease and hepatocellular carcinoma progression. Cytokine 2019; 124: 154569.

[30] Wang F, Zhang X, Liu W, Zhou Y, Wei W, Liu D, Wong CC, Sung JJY and Yu J. Activated natural killer cell promotes nonalcoholic steatohepatitis through mediating JAK/STAT pathway. Cell Mol Gastroenterol Hepatol 2022; 13: 257-274.

[31] Yao Y, Luo ZP, Li HW, Wang SX, Wu YC, Hu Y, Hu S, Yang CC, Yang JF, Wang JP, Peng L, Chen F, Pan LX and Xu T. P38γ modulates the lipid metabolism in non-alcoholic fatty liver disease by regulating the JAK-STAT signaling pathway. Faseb J 2023; 37: e22716.